



## Research paper

# Verification of punching shear outside the shear cap by the direct method

Maciej Grabski<sup>1</sup>, Andrzej Ambroziak<sup>2</sup>

**Abstract:** The proposition of a method to verify the punching resistance for very large supports based on the EN 1992-1-1 standard is described in this paper. The present standard guidelines for the calculation of the punching resistance for large supports are also summarised. The proposed direct method is compared with other standard methods using an example taken from design practice. This method consists of a direct check of the shear forces at specific locations of the control perimeter with the permissible shear force calculated from the EC2 standard. The method showed very good agreement with the experiment while remaining practical for applications. The method presented takes into account the actual distribution of shear forces in the vicinity of the support, taking into account the influence of non-uniform loads, irregular floor geometry, the concentration of internal forces at the corners of the support and the influence of the stiffness of the head used. The paper provides scientists, engineers, and designers new method (called the direct method) for estimation of the punching load-bearing capacity outside the shear cap.

**Keywords:** punching shear, shear cup, direct method, slab-column, RC slab

<sup>1</sup>MSc, Maciej Grabski Engineering, 94B/1 Leszczynowa Street, 80-175 Gdańsk, Poland, e-mail: [grabski@engineering.pl](mailto:grabski@engineering.pl), ORCID: 0000-0002-4765-4007

<sup>2</sup>DSc., PhD., Eng., Prof. GUT, Gdansk University of Technology, Faculty of Civil and Environmental Engineering, St. Gabriela Narutowicza 11/12, 80-233 Gdańsk, Poland, e-mail: [ambrozan@pg.edu.pl](mailto:ambrozan@pg.edu.pl), ORCID: 0000-0002-7735-7863

## 1. Introduction

The rapid growth of reinforced concrete construction in the second half of the 19th century was responsible for the appearance of many innovative structural systems throughout the world [1]. The first slab-column structures appeared almost at the same time in different countries. One of the first inventors of mushroom head structures was Claude A.P. Turner, who designed and built his first building in this technology in 1906 [2]. The earliest slab-column construction in Europe was built by Robert Maillart [3]. At the same time, Artur Ferdinandovitch Loleit carried out his work on the mushroom system [4]. All early structural systems included an enlarged column head at the connection between the column and the slab. This was an intuitive solution to the zone where the maximum stresses were located. The popularity of slab-column structures and the complexity of the punching shear issue make this topic a research subject of many investigations [5–10]. The improper design of the slab-column structures may collapse due to the phenomenon of punching [11, 12]. Many parameters influence punching shear resistance, e.g., type and strength of concrete [13–15], support shape and dimension [16–18], quantity and distribution of longitudinal and transverse reinforcement [19–23], membrane effect [24, 25], the effect of the hole near to support [26, 27], cyclic load [28, 29], type of concrete [9, 30], shear slenderness [31]. Despite the possibility of reinforcing the slab-column joint with various types of steel inserts [32–34] the use of slab thickening near point support is still common. The advantage of this type of strengthening is to increase the punching resistance and at the same time increase the stiffness of the slab. Numerous studies are carried out also on the structure after its failure as a result of punching shear [35–38] or strengthening against punching shear [39–42].

The design process for a slab-column connection topped with a head requires verification of the punching resistance in the head zone and the slab zone outside the head. Considering punching outside the head area is most often dealing with the case of large flexible support with a rectangular shape, Fig. 1. For large or elongated supports the distribution of shear forces near the support is uneven despite symmetrical loading [43–45], Fig. 2. Stress concentrations at corners contribute to a reduction in punching shear resistance. The issue of punching outward of the head, the stiffness of the head is an important parameter affecting the force concentrations at the corners of the support and the resistance of the connection [46, 47].

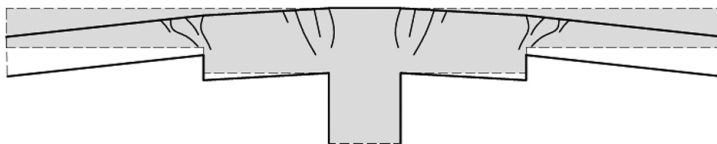


Fig. 1. Shear head as a flexible slab support

The proposal for a method to verify the punching resistance of very large supports based on the EN 1992-1-1 (EC2) [48] standard is given. The present standard guidelines

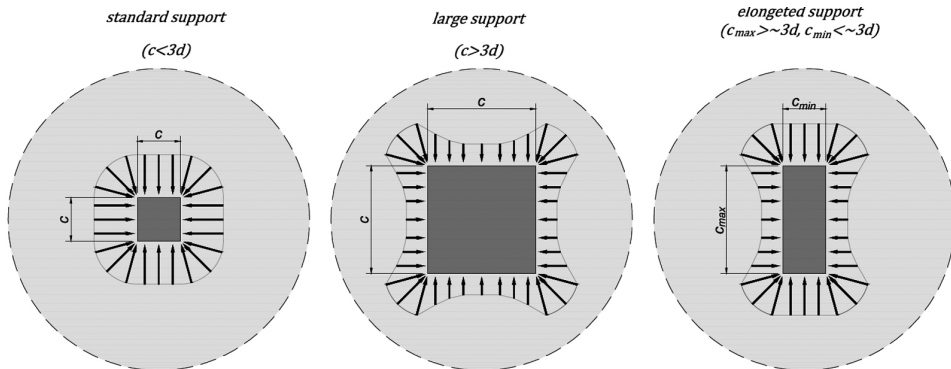


Fig. 2. Distribution of shear forces in the internal support zone as a function of its size and shape concerning the effective slab height ( $d$ )

for the calculation of the punching resistance for very large supports are also summarised. The proposed method is compared with other standard methods using an example taken from design practice.

## 2. Building standards

In most codes of practice, the punching strength of a slab-column connection is verified by comparing a nominal shear stress per unit length of the control perimeter  $v_E$  to the permissible shear stress of the element  $v_R$ , as:

$$(2.1) \quad v_E = \frac{V}{b_0 \cdot d} \leq v_R$$

where:  $V$  – punching force,  $b_0$  – length of the control perimeter,  $d$  – effective slab height.

Therefore, the influence of the load area size on the punching resistance depends on a way to calculate the permitted shear stress and the location of the control perimeter. The different parameters taken into account to calculate the permissible stresses and the different locations of the control perimeter cause the influence of column size on punching capacity to vary depending on the code used. In the EC2 [48] a non-uniform distribution of shear forces is accounted for by increasing the acting shear stresses by a factor  $\beta > 1.0$  which is a function of the moment transfer between the slab and the column. The EC2 standard lacks recommendations for elongated or large load areas. Some European countries have added restrictions on the punching for large supports in national annexes – for example, EC2-DIN [49] provides a limitation on the length of the control perimeter, Fig. 3b.

The ACI318 [50] code takes this effect into account by reducing the allowable shear stresses depending on the size and shape of the support, Table 1. The MC2010 [51] standard



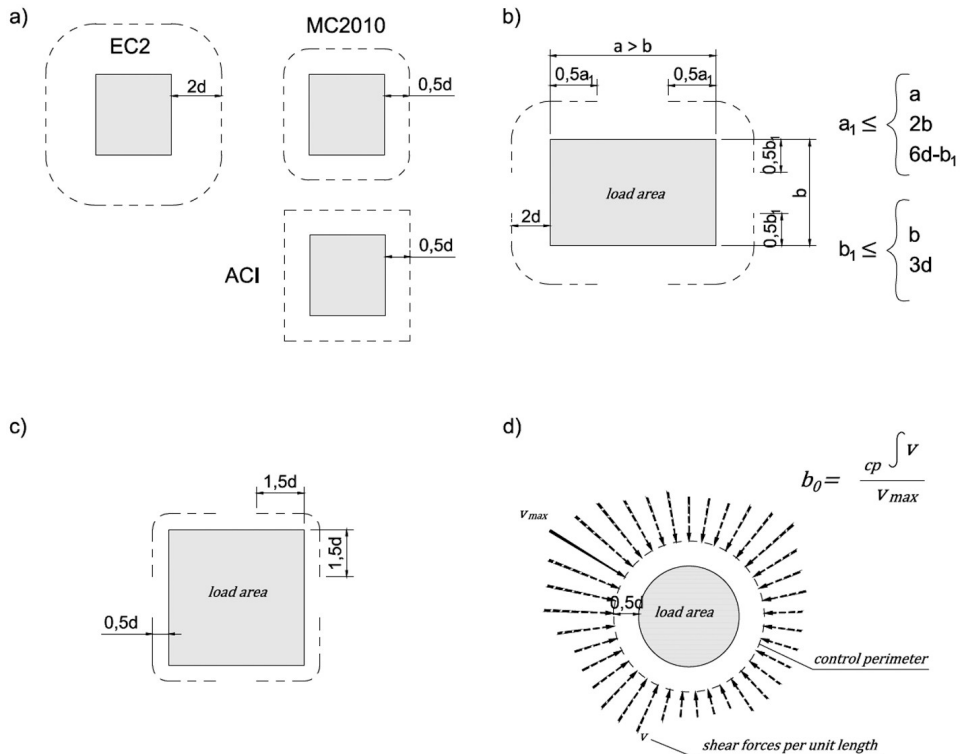


Fig. 3. Control perimeter: a) basic according to EC2, MC2020 and ACI standards; b) EC2-DIN reduction; c) MC2020-simplified method reduction; d) MC2020-general method reduction

adopts a method for reducing the control perimeter. Introduces a simplified method that reduces the control perimeter according to Fig. 3c or a general method that reduces the length of the control perimeter based on the actual distribution of cutting forces in the control perimeter

$$(2.2) \quad b_{0,eff} = \frac{V}{v_{max}}$$

where:  $b_{0,eff}$  – length of the shear control perimeter,  $v_{max}$  – maximum value of the shear force per unit length along the perimeter, Fig. 3d.

In addition, the length of the examined section must be reduced by a factor that takes account of the effect of the bending moment on the shear stress in the control section. The basic calculation formulae according to EC2 [48], MC2010 [51] and ACI [50] standards are presented in Table 1.



Table 1. Summary of the methodology to estimate the slab punching shear resistance

	Actual stresses ( $v_E$ )	Permissible stresses ( $v_R$ )
EC2 [48] / EC2-DIN [49]	$v_{E,i} = \beta \cdot \frac{V}{b_i \cdot d}$ $\beta = 1 + 1.8 \cdot \sqrt{\left(\frac{e_1}{b_2}\right)^2 + \left(\frac{e_2}{b_1}\right)^2}$ $b_i = b_{0,EC2}; b_{0,EC2-DIN}$ $v_{E,i} = v_{E,EC2}; v_{E,EC2-DIN}$	$v_{R,EC2} = \frac{0.18}{\gamma_c} \cdot k \cdot \sqrt[3]{100 \cdot \rho_l \cdot f_{ck}} \geq v_{\min}$ $k = 1 + \sqrt{200/d} \leq 2$ $\rho_l = \sqrt{\rho_{l1} \cdot \rho_{l2}} \leq 0.02$ $v_{\min} = 0.035 \cdot k^{3/2} \cdot f_{ck}^{1/2}$
ACI318 [50]	$v_{E,ACI} = \frac{V}{b_{0,ACI} \cdot d}$ $+ \frac{\gamma_v \cdot M_{Ed} \cdot c_{AB}}{J_c}$	$v_{R,ACI} = \Phi \cdot \min \begin{cases} 0.332 \cdot \sqrt{f_{ck}} \\ 0.083 \cdot \left(2 + \frac{4}{\beta_A}\right) \cdot \sqrt{f_{ck}} \\ 0.083 \cdot \left(2 + \frac{\alpha_s \cdot d}{b_0}\right) \cdot \sqrt{f_{ck}} \end{cases}$ $\beta_A = c_1 / c_2 \geq 1.0$ $\alpha_s = 40$
MC2010 [51]	$v_{E,i} = \frac{V}{k_e \cdot b_i \cdot d}$ $b_i = b_{0,MC}; b_{0,MC,eff}; b_{0,MC,3d}$ $v_{E,i} = v_{E,MC}; v_{E,MC,eff}; v_{E,MC,3d}$	$v_{R,MC} = \frac{k_\psi}{\gamma_c} \cdot \sqrt{f_{ck}}$ $k_\psi = \frac{1}{1.5 + 0.9 \cdot k_{dg} \cdot \psi \cdot d} \leq 0.6$ $k_{dg} = \frac{32}{16 + d_g} \geq 0.75$ $\psi = 1.2 \cdot \frac{r_s \cdot f_{yd}}{d \cdot E_s} \cdot \left(\frac{m_{Ed}}{m_{Rd}}\right)^{1.5}$

### 3. Direct method description

The proposed method for calculating the resistance of the connection according to the EC2 [48] is the verification method called the direct method. This method is recommended for checking the resistance of large supports. The direct method assumes separating for the large support ( $c/d > 4$ ) type 1 sections which have to be checked for two-way shear and type 2 sections which have to be checked according to the rules for one-way shear, Fig. 4.

The EC2 [48] formula for permissible shear stresses in the control section is the same for shear and punching shear, it is proposed to perform the check by comparing the existing shear forces in the slab with the permissible shear forces calculated based on EC2, Table 1.

The general verification condition can be described as:

$$(3.1) \quad v_E = \frac{V}{b_0} \leq v_R \cdot d.$$

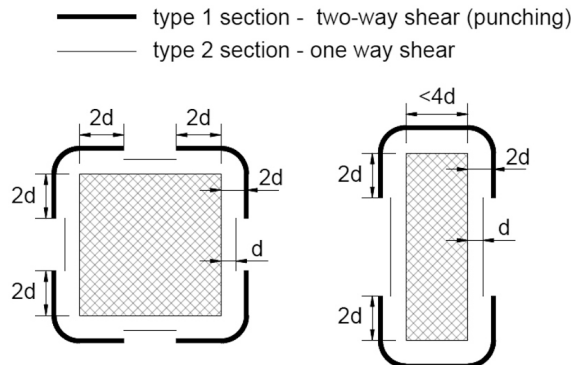


Fig. 4. Separate sections for checking two-way shear and one-way shear

The left part of the equation (3.1) can be replaced by the actual shear force calculated in the finite element method (FEM) design model:

$$(3.2) \quad v_{\max, \text{FEM}} \leq v_R \cdot d,$$

where:

$$v_{\max, \text{FEM}} = \sqrt{v_{\max, \text{FEM}, x}^2 + v_{\max, \text{FEM}, y}^2}$$

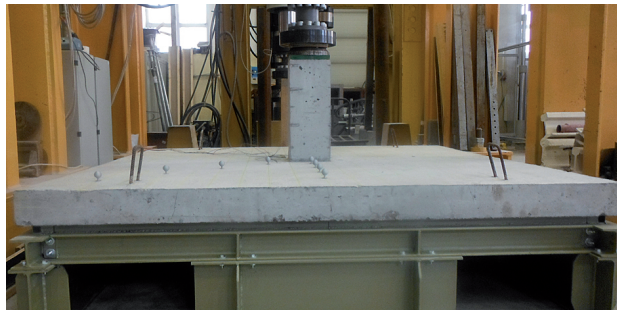
The force  $v_{\max, \text{FEM}}$  should be derived as a maximum transverse force from type 1 or type 2 sections. As it can be seen in Fig. 4, the difference in checking the resistance condition between sections of type 1 and type 2 is the control cross-section in which the force is taken from the FEM design model. According to the EC2 [48], in the case of linear shear, the control section is located at a distance  $d$  from the support, whereas in the case of punching shear it is located at a distance  $2d$  from the support.

The direct method, which can be used in design practice, requires the development of a computational model. In addition, available calculation programs can directly read the main shear force in the floor slab, so it can be concluded that the method is practical. In addition, an advantage of the notation of the ultimate condition is that it is easily adaptable to other design standard methods. In the case of other design methods, the calculation of  $v_R$  and the location of the control sections from which the shear force is derived changes. When punching shear reinforcement is required, the provisions related to the standard used must be applied. In this case, the sections are special cases of calculation: wall corner, wall end, linear shear.

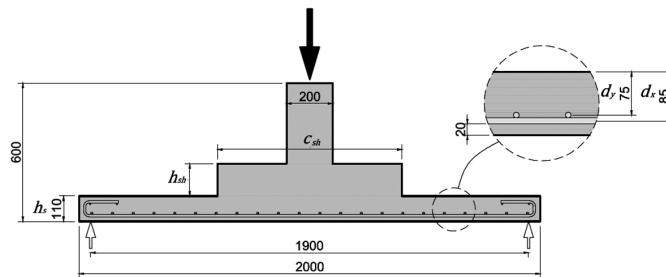
## 4. Comparison with experimental results

The proposed direct method was verified based on experimental punching shear tests [47]. The tested members (Fig. 5) were a slab-column reinforced concrete element with a column topped by a shear head (dented G1-300, G2-400, G3-600, G4-800, and

G5-900, where the number indicates dimensions of the shear heads) and without a shear head (denoted S1-200). Square slabs were  $200 \times 200$  cm and 11 cm in total height. The column dimension for each tested element was  $200 \times 200$  mm. The height of the shear head was 240 mm. The concrete slabs were reinforced with orthogonal ribbed bars of 10 mm diameter at 90 mm spacing.



(a)



(b)

Fig. 5. Slab-column elements: (a) laboratory test stand, (b) cross-section

For tested members named S1-200, G1-300, G2-400, G3-600, G4-800, and G5-900, computational models were created to represent the behaviour of each concrete element, Fig. 6a. The numerical models were loaded with the ultimate forces registered during performed experimental tests, Fig. 6d and Fig. 7. In the calculations of the test elements, it was also considered to replace the maximum force with the average force of the section under consideration (type 1 or type 2). The results of the calculation are shown in Table 2 and Table 3. The calculations carried out by the direct method show an average coefficient of load punching capacity for type 1 sections of the test elements equal to 1.12 with a coefficient of variation equal to 0.08. When the average transverse force is applied, the average resistance factor, in this case, is 1.03 with a standard deviation of 0.05. The calculations confirm the very good fit of the direct method with the experimental results. Type 2 sections did not show high strain, which is also consistent with the test observations (full breakthrough in corners and partial breakthrough in straight sections of elements G4-800 and G5-900). Despite the better test fit of the average force method variant, it



is recommended for the EC2-based method to use the maximum force due to the small number of tests performed in the range of very large supports. A calculation example of the test element G4-800 is presented in Figs. 6 and 7.

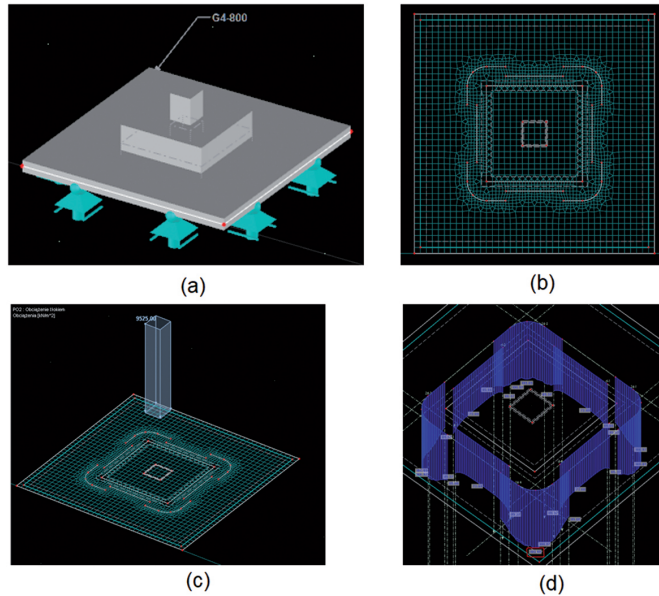


Fig. 6. FEM computational model of G4-800 element: (a) visualisation; (b) finite element mesh; (c) loading; (d) shear force diagrams

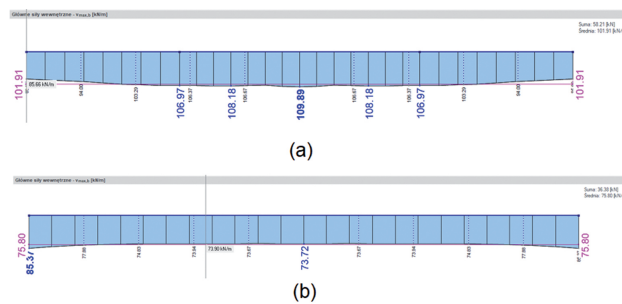


Fig. 7. Shear force diagrams in G4-800 element: (a) type 1 section –  $v_{\max, \text{FEM}} = 109.9 \text{ kN/m}$ ,  $v_{\text{av}, \text{FEM}} = 101.9 \text{ kN/m}$ ; (b) type 2 section –  $v_{\max, \text{FEM}} = 85.4 \text{ kN/m}$ ,  $v_{\text{av}, \text{FEM}} = 75.8 \text{ kN/m}$

The permissible transverse stresses can be calculated as:

$$(4.1) \quad v_{R,c} = C_{R,c} \cdot k \cdot \sqrt[3]{100 \cdot \rho_l \cdot f_{ck}} = 0.18 \cdot 2 \cdot \sqrt[3]{100 \cdot 0.011 \cdot 38.14} = 1.25 \text{ MPa}$$

$$v_{R,c} = 1.25 \text{ MPa} \geq 0.035 \cdot k^{3/2} \cdot f_{ck}^{1/2} = 0.035 \cdot 2^{3/2} \cdot 38.14^{1/2} = 0.61 \text{ MPa}$$





while permissible shear force in type 1 and type 2 sections is:

$$(4.2) \quad v_{R,c} \cdot d = 0.125 \cdot 8 = 1 \frac{\text{kN}}{\text{cm}}$$

Table 2. Calculation of ultimate punching capacity condition by direct method – sections type 1

Test element	$v_{\max, \text{FEM}}$ [kN/m]	$v_{\text{av}, \text{FEM}}$ [kN/m]	$v_{R,c \text{ EC2}}$ [kN/m]	$v_{\max, \text{MES}} / v_{R,c \text{ EC2}}$ [-]	$v_{\text{av}, \text{MES}} / v_{R,c \text{ EC2}}$ [-]
S1-200	92.3	89.5	96.5	0.96	0.93
G1-300	120.0	108.5	98.6	1.22	1.10
G2-400	111.3	97.9	96.8	1.15	1.01
G3-600	115.0	103.5	97.9	1.17	1.06
G4-800	109.9	101.9	100.1	1.10	1.02
G5-900	105.7	100.5	94.7	1.12	1.06
			Mean	1.12	1.03

Table 3. Calculation of ultimate capacity condition by direct method – sections type 2

Test element	$v_{\max, \text{FEM}}$ [kN/m]	$v_{\text{av}, \text{FEM}}$ [kN/m]	$v_{R,c \text{ EC2}}$ [kN/m]	$v_{\max, \text{MES}} / v_{R,c \text{ EC2}}$ [-]	$v_{\text{av}, \text{MES}} / v_{R,c \text{ EC2}}$ [-]
S1-200	–	–	96.5	–	–
G1-300	–	–	98.6	–	–
G2-400	54.1	50.0	96.8	0.56	0.52
G3-600	68.1	56.4	97.9	0.70	0.58
G4-800	85.4	75.8	100.1	0.85	0.76
G5-900	83.6	79.7	94.7	0.88	0.84
			Mean	0.73	0.66

## 5. Constructional calculation example

A two-storey car park structure with irregular column spacing (Fig. 8) is analysed for punching shear outside the column head. The connection between the floor slab and the column topped with a head is analysed. The column dimension is  $65 \times 35$  cm. The slab thickness is 24 cm (effective high  $d = 20$  cm) and the head thickness is 55 cm. Within the shear cap area, a thickened surface was added, which is placed eccentrically concerning the slab so that the upper surfaces of both slabs are on the same level. The structure is



designed with C35/45 concrete class and reinforced by steel bars with a yield strength  $f_y = 500$  MPa. The maximum aggregate size is 16 mm. The applied reinforcement in the X and Y direction is  $10.05 \text{ cm}^2/\text{m}$  and  $20.11 \text{ cm}^2/\text{m}$ , respectively. The 3D shell finite element analysis is performed in the RFEM program of Dlubal Software. The program can present the main shear forces in the cross-section of the control perimeter or any other cross-section modelled by the user. The numerical results are obtained in the linear elastic analysis by modelling the slab as a shell element using finite elements of the MITC type (Mixed Interpolation of Tensorial Components [52, 53]). The finite element (FE) mesh convergence study of the slab–column–connection FE model is carried out to ensure that the results of an analysis are not affected by changing the size of the FE mesh. The total design load uniformly distributed is 14.75 kPa. The forces acting in the column from the applied load are shown in Fig. 9.

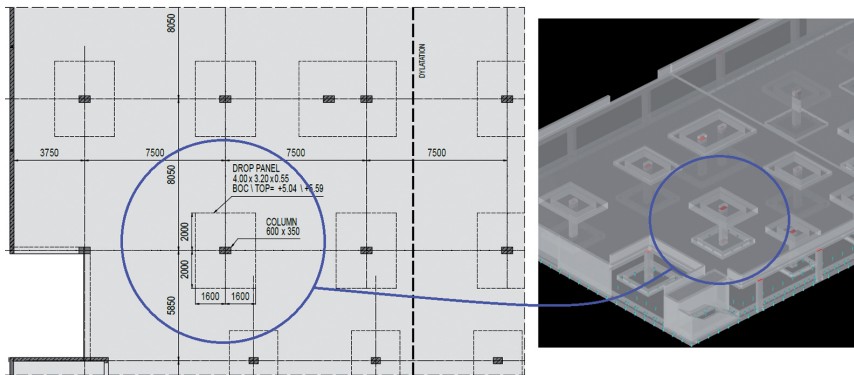


Fig. 8. View on slab-column structure

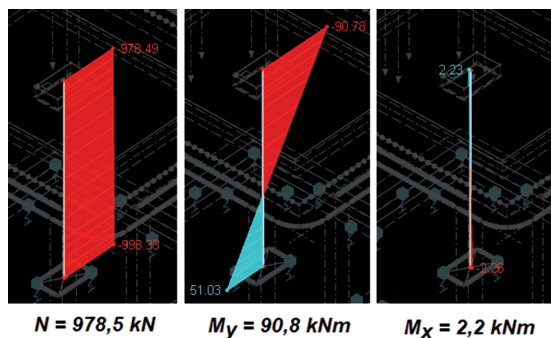


Fig. 9. Forces at the chosen column

Table 4 shows the punching shear calculations in the region outside the column head. The calculation takes into account the calculation methods collected in Table 1. An alternative verification with the proposed direct method is shown in Table 5. The forces derived from the computational model are shown in Figs. 10–12.



Table 4. Calculation results of the described standard methods

	Stresses in the joint ( $v_E$ )	Permissible stresses in the joint ( $v_R$ )
EC2 [48]/ EC2- DIN [49]	$v_{E,EC2} = 1.03 \cdot \frac{978.5}{16.91 \cdot 0.2} \cdot 10^{-3}$ = 0.30 MPa	$v_{R,EC2} = \frac{0.18}{1.5} \cdot 2 \cdot \sqrt[3]{100 \cdot 0.0071 \cdot 35}$ = 0.70 MPa $v_{R,EC2} = 0.70 \text{ MPa} \geq v_{\min} = 0.59 \text{ MPa}$
	$v_{E,EC2-DIN} = 1.03 \cdot \frac{978.5}{4.91 \cdot 0.2} \cdot 10^{-3}$ = 1.03 MPa	
ACI318 [50]	$v_{E,ACI} = \left( \frac{978.5}{15.2 \cdot 0.2} + \frac{0.37 \cdot 90.8 \cdot 1.7}{6.17} \right) \cdot 10^{-3}$ = 0.33 MPa	$v_{R,ACI} = 0.75 \cdot \min \begin{cases} 0.332 \cdot \sqrt{35} \\ 0.083 \cdot \left( 2 + \frac{4}{1.25} \right) \cdot \sqrt{35} \\ 0.083 \cdot \left( 2 + \frac{40 \cdot 0.2}{15.2} \right) \cdot \sqrt{35} \end{cases}$ $v_{R,ACI} = 0.93 \text{ MPa}$
MC2010 [51]	$v_{E,MC} = \frac{978.5}{0.98 \cdot 15.02 \cdot 0.2} \cdot 10^{-3}$ = 0.33 MPa	$\psi = 1.2 \cdot \frac{2.34 \cdot 434.8}{0.2 \cdot 200\,000} \cdot \left( \frac{32.0}{80.1} \right)^{1.5}$ = 0.008 rad $k_\psi = \frac{1}{1.5 + 0.9 \cdot 1 \cdot 0.008 \cdot 200}$ = 0.34 ≤ 0.6 $v_{R,MC} = \frac{0.34}{1.5} \cdot \sqrt{35} = 1.34 \text{ MPa}$
	$v_{E,MC,3d} = \frac{978.5}{0.98 \cdot 3.02 \cdot 0.2} \cdot 10^{-3}$ = 1.65 MPa	
	$b_{0,MC,eff} = \frac{978.5}{137.93} = 7.09 \text{ m}$ $v_{E,MC,eff} = \frac{978.5}{0.98 \cdot 7.09 \cdot 0.2} \cdot 10^{-3}$ = 0.70 MPa	

Table 5. Results of the direct method calculations

Section	Maximum shear force in sections ( $v_{\max,FEM}$ )	Permissible shear force in sections ( $v_R \cdot d$ )
L1	$v_{\max,FEM} = 54.42 \text{ kN/m}$	$v_{R,EC2} \cdot d = 126 \text{ kN/m}$
L2	$v_{\max,FEM} = 25.66 \text{ kN/m}$	$v_{R,EC2} \cdot d = 155 \text{ kN/m}$
L3	$v_{\max,FEM} = 44.94 \text{ kN/m}$	$v_{R,EC2} \cdot d = 126 \text{ kN/m}$
L4	$v_{\max,FEM} = 35.62 \text{ kN/m}$	$v_{R,EC2} \cdot d = 155 \text{ kN/m}$
C1	$v_{\max,FEM} = 50.42 \text{ kN/m}$	$v_{R,EC2} \cdot d = 140 \text{ kN/m}$
C2	$v_{\max,FEM} = 57.04 \text{ kN/m}$	$v_{R,EC2} \cdot d = 140 \text{ kN/m}$
C3	$v_{\max,FEM} = 43.71 \text{ kN/m}$	$v_{R,EC2} \cdot d = 140 \text{ kN/m}$
C4	$v_{\max,FEM} = 41.43 \text{ kN/m}$	$v_{R,EC2} \cdot d = 140 \text{ kN/m}$



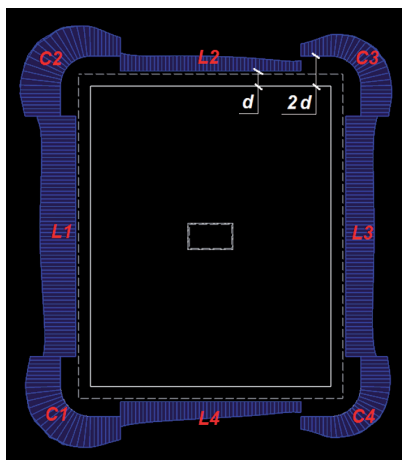


Fig. 10. Distributions of shear force in control sections of the direct method.  
General view and designation of individual sections

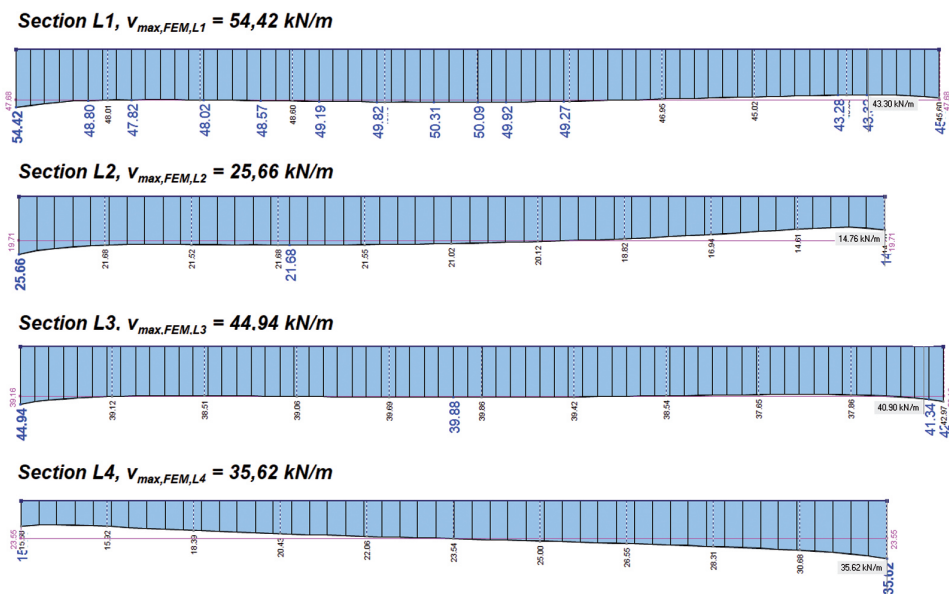
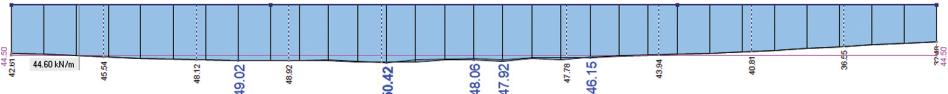


Fig. 11. Shear force distributions in 2<sup>nd</sup> type sections

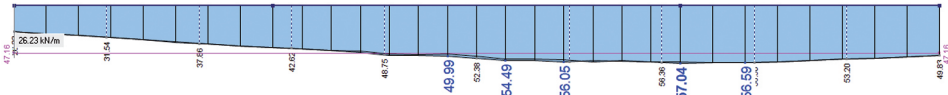
The presented results of the calculations vary considerably depending on the calculation method used, Fig. 13.

According to chosen standard calculation methods, the key factor influencing the load-bearing punching capacity of a slab-column joint is the assumed length of the control perimeter. The final result of the resistance calculation is very sensitive to this parameter.

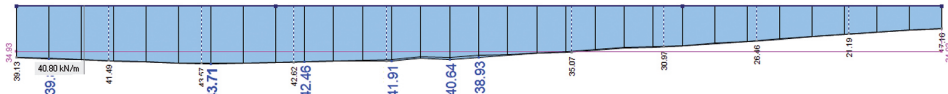
**Section C1,  $v_{max,FEM,C1} = 50,42$  kN/m**



**Section C2,  $v_{max,FEM,C2} = 57,04$  kN/m**



**Section C3,  $v_{max,FEM,C3} = 43,71$  kN/m**



**Section C4,  $v_{max,FEM,C4} = 41,43$  kN/m**

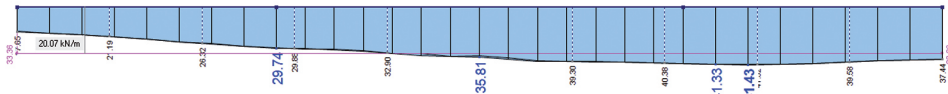


Fig. 12. Shear force distributions in 1<sup>st</sup> type sections

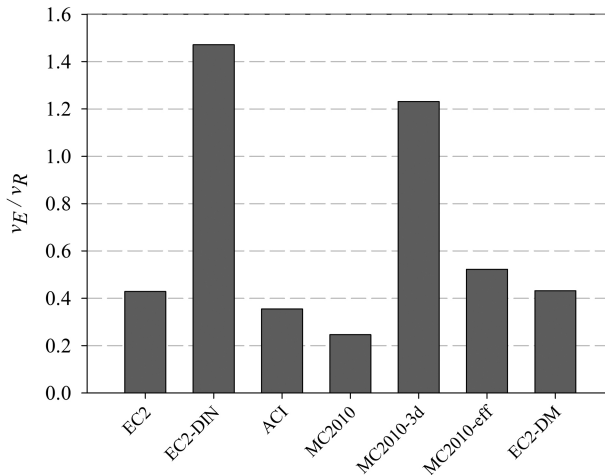


Fig. 13. Punching load capacity conditions – standard methods comparison

Experimental studies [47] have shown that for very large supports, methods that reduce the control circuit (EC2-DIN, MC2010-3d) lead to unreasonable results. The proposed method for direct checking of cutting forces eliminates the problem of determining the length of the control perimeter. Presented calculation results confirm a very good agreement of the method with experimental studies.

## 6. Conclusions

Based on the EC2 standard, the authors of this paper propose a direct method for checking the punching resistance condition for large support dimensions. This method consists of a direct check of the shear forces at specific locations of the control perimeter with the permissible shear force calculated from the EC2 standard. The presented calculation example demonstrates the significant advantage of taking into account the non-uniform distribution of shear forces acting around the joint by taking into account the influence of non-uniform loads, slab geometry, the concentration of internal forces at the corners of the support and the influence of the stiffness of the shear head used. The method showed very good agreement with the performed experiments while remaining practical for applications. Nevertheless, it seems necessary to carry out a large number of laboratory tests to prove the universality of the proposed method. The method presented takes into account the actual distribution of shear forces in the vicinity of the support, taking into account the influence of non-uniform loads, irregular floor geometry, the concentration of internal forces at the corners of the support and the influence of the stiffness of the head used. This is another advantage of the proposed method compared to standard methods for calculating the punching resistance outside the shear heads. The authors of this paper hope that the proposed method will be helpful to structural designers in assessing the actual punching resistance of slab-to-column connections topped with a shear head.

## References

- [1] M. Moussard, P. Garibaldi, M. Curbach, "The invention of Reinforced concrete (1848-1906)", in *High Tech Concrete: Where Technology and Engineering Meet – Proceedings of the 2017 fib Symposium, 2017*. Maastricht, The Netherlands: Springer, 2017, pp. 2785–2794; DOI: [10.1007/978-3-319-59471-2\\_316](https://doi.org/10.1007/978-3-319-59471-2_316).
- [2] A. Kierdorf, "Early Mushroom Slab Construction in Switzerland, Russia and the U.S.A. – A Study in Parallel Technological Development", in *Proceedings of the Second International Congress on Construction History*. Cambridge, 2006, pp. 1793–1807. [Online]. Available: <https://www.arct.cam.ac.uk/system/files/documents/vol-2-1793-1808-kierdorf.pdf>.
- [3] A.S. Saadon, A.M. Abbas, H.K. Hussain, "A Review on Flat Slab Punching Shear Reinforcement", *Journal of University of Babylon for Engineering Sciences*, 2019, vol. 27, no. 3, pp. 44–58.
- [4] L. Slivnik, "The Distinction between Mushroom and Umbrella Structures in Slovene Architecture", *IOP Conference Series: Materials Science and Engineering*, 2019, vol. 471, no. 8, art. ID 082058; DOI: [10.1088/1757-899X/471/8/082058](https://doi.org/10.1088/1757-899X/471/8/082058).
- [5] M. Gołdyn, T. Urban, "Hidden capital as an alternative method for increasing punching shear resistance of LWCA flat slabs", *Archives of Civil Engineering*, 2019, vol. 65, no. 4, pp. 309–328; DOI: [10.2478/ace-2019-0062](https://doi.org/10.2478/ace-2019-0062).
- [6] A. Ambroziak, M. Grabski, "Analiza porównawcza metod obliczania przebiccia", *Materiały Budowlane*, 2019, vol. 563, no. 7, pp. 52–55; <https://www.materiaלבudowlane.info.pl/zintegrowane-projektowanie-410/418-wydanie/mb-07-2019/12183-analiza-porownawcza-metod-obliczania-przebiccia.html>.
- [7] A. Ambroziak, M. Grabski, "Sposoby przykładania obciążenia zmiennego na konstrukcję płytowo-słupową", *Materiały Budowlane*, 2019, vol. 557, no. 1, pp. 80–82; DOI: [10.15199/33.2019.01.15](https://doi.org/10.15199/33.2019.01.15).
- [8] M. Grabski, A. Ambroziak, "Shear cap size selection method based on parametric analysis of ACI-318 code and Eurocode 2 standard", *Materials (Basel)*, 2020, vol. 13, no. 21, pp. 1–24; DOI: [10.3390/ma13214938](https://doi.org/10.3390/ma13214938).
- [9] M. Gołdyn, Ł. Krawczyk, W. Ryżyński, T. Urban, "Experimental investigations on punching shear of flat slabs made from lightweight aggregate concrete", *Archives of Civil Engineering*, 2018, vol. 64, no. 4/I, pp. 293–306; DOI: [10.2478/ace-2018-0058](https://doi.org/10.2478/ace-2018-0058).



- [10] T. Urban, M. Gołdyn, L. Krawczyk, “Strengthening of RC slabs against punching shear in theory and practice”, *Archives of Civil Engineering*, 2021, vol. 67, no. 4, pp. 317–335; DOI: [10.24425/ace.2021.138502](https://doi.org/10.24425/ace.2021.138502).
- [11] J. Halvoník, A. Vidaković, V. Borzovič, “Failure analysis of collapsed parking garage building due to punching”, *Engineering Failure Analysis*, 2021, vol. 129, art. ID 105712; DOI: [10.1016/j.engfailanal.2021.105712](https://doi.org/10.1016/j.engfailanal.2021.105712).
- [12] S. King, N.J. Delatte, “Collapse of 2000 Commonwealth Avenue: Punching Shear Case Study”, *Journal of Performance of Constructed Facilities*, 2004, vol. 18, no. 1, pp. 54–61; DOI: [10.1061/\(ASCE\)0887-3828\(2004\)18:1\(54\)](https://doi.org/10.1061/(ASCE)0887-3828(2004)18:1(54)).
- [13] H. Marzouk, A. Hussein, “Experimental investigation on the behavior of high-strength concrete slabs”, *Structural Journal*, 1991, vol. 88, no. 6, pp. 701–713.
- [14] M.M.G. Inácio, A.F.O. Almeida, D.M.V. Faria, et al., “Punching of high strength concrete flat slabs without shear reinforcement”, *Engineering Structures*, 2015, vol. 103, pp. 275–284; DOI: [10.1016/j.engstruct.2015.09.010](https://doi.org/10.1016/j.engstruct.2015.09.010).
- [15] M.M.G. Inácio, M. Lapi, A. Pinho Ramos, “Punching of reinforced concrete flat slabs – Rational use of high strength concrete”, *Engineering Structures*, 2020, vol. 206, art. ID 110194; DOI: [10.1016/j.engstruct.2020.110194](https://doi.org/10.1016/j.engstruct.2020.110194).
- [16] J. Sagaseta, L. Tassinari, M. Fernández Ruiz, A. Muttoni, “Punching of flat slabs supported on rectangular columns”, *Engineering Structures*, 2014, vol. 77, pp. 17–33; DOI: [10.1016/j.engstruct.2014.07.007](https://doi.org/10.1016/j.engstruct.2014.07.007).
- [17] D.R.C. Oliveira, P.E. Regan, G.S.S.A. Melo, “Punching resistance of RC slabs with rectangular columns”, *Magazine of Concrete Research*, 2004, vol. 56, no. 3, pp. 123–138; DOI: [10.1680/macr.2004.56.3.123](https://doi.org/10.1680/macr.2004.56.3.123).
- [18] N.M. Hawkins, H.B. Fallsen, R.C. Hinojosa, “Influence of column rectangularity on the behavior of flat plate structures”, *ACI Journal & Proceedings*, 1972, vol. 69, no. 1, pp. 127–146.
- [19] S. Guandalini, O.L. Burdet, A. Muttoni, “Punching tests of slabs with low reinforcement ratios”, *Structural Journal*, 2009, vol. 106, no. 1, pp. 87–95.
- [20] S. Lips, “Punching of flat slabs with large amounts of shear reinforcement”, Ph.D. thesis, École Polytechnique Fédérale de Lausanne, Switzerland, 2012. [Online]. Available: [https://infoscience.epfl.ch/record/180221/files/EPFL\\_TH5409.pdf](https://infoscience.epfl.ch/record/180221/files/EPFL_TH5409.pdf).
- [21] P. Schmidt, D. Kueres, J. Hegger, “Punching shear behavior of reinforced concrete flat slabs with a varying amount of shear reinforcement”, *Structural Concrete*, 2020, vol. 21, no. 1, pp. 235–246; DOI: [10.1002/suco.201900017](https://doi.org/10.1002/suco.201900017).
- [22] B. Wieczorek, W. Starosolski, “Wpływ mimośrodowego obciążenia na nośność połączenia płyta-słup po przebiegu”, *Zeszyty Naukowe Politechniki Rzeszowskiej. Budownictwo i Inżynieria Środowiska*, 2012, vol. 59, no. 3/II, pp. 133–140. [Online]. Available: [https://oficyna.prz.edu.pl/fcp/NGBUKOQfTKIQhbx08SlkAWxhQAYkrCDILDWdbE1VGWGFbWxslAxtlFSVcVnRKCKI8VQIDJCUODBYAKg8TXBEbIRBSBw/18/public/zeszyty\\_naukowe/wbiis/2012/budownictwo-pw-nowe/bud-59-03-2-pw2.pdf](https://oficyna.prz.edu.pl/fcp/NGBUKOQfTKIQhbx08SlkAWxhQAYkrCDILDWdbE1VGWGFbWxslAxtlFSVcVnRKCKI8VQIDJCUODBYAKg8TXBEbIRBSBw/18/public/zeszyty_naukowe/wbiis/2012/budownictwo-pw-nowe/bud-59-03-2-pw2.pdf).
- [23] P.M. Lewiński, P.P. Więch, “Finite element model and test results for punching shear failure of RC slabs”, *Archives of Civil and Mechanical Engineering*, 2020, vol. 20, no. 2, pp. 1–16; DOI: [10.1007/s43452-020-00037-x](https://doi.org/10.1007/s43452-020-00037-x).
- [24] B. Belletti, J.C. Walraven, F. Trapani, “Evaluation of compressive membrane action effects on punching shear resistance of reinforced concrete slabs”, *Engineering Structures*, 2015, vol. 95, pp. 25–39; DOI: [10.1016/j.engstruct.2015.03.043](https://doi.org/10.1016/j.engstruct.2015.03.043).
- [25] J. Einpaul, M. Fernández Ruiz, A. Muttoni, “Influence of moment redistribution and compressive membrane action on punching strength of flat slabs”, *Engineering Structures*, 2015, vol. 86, pp. 43–57; DOI: [10.1016/j.engstruct.2014.12.032](https://doi.org/10.1016/j.engstruct.2014.12.032).
- [26] S. Teng, H.K. Cheong, K.L. Kuang, J.Z. Geng, “Punching Shear Strength of Slabs with Openings and Supported on Rectangular Columns”, *Structural Journal*, 2004, vol. 101, no. 5, pp. 678–687.
- [27] M. Gołdyn, T. Urban, “The effect of openings size and location on the punching shear carrying capacity of the support zones of flat slabs in the light of the existing experimental investigations”, *Inżynieria i Budownictwo*, 2019, vol. 75, no. 4, pp. 165–170.
- [28] A.F.O. Almeida, M.M.G. Inácio, V.J.G. Lúcio, A.P. Ramos, “Punching behaviour of RC flat slabs under reversed horizontal cyclic loading”, *Engineering Structures*, 2016, vol. 117, pp. 204–219; DOI: [10.1016/j.engstruct.2016.03.007](https://doi.org/10.1016/j.engstruct.2016.03.007).



- [29] I. Robertson, G. Johnson, "Cyclic lateral loading of nonductile slab-column connections", *Structural Journal*, 2006, vol. 103, no. 3, pp. 356–364.
- [30] T. Urban, M. Gołdyn, Ł. Krawczyk, Ł. Sowa, "Experimental investigations on punching shear of lightweight aggregate concrete flat slabs", *Engineering Structures*, 2019, vol. 197, art. ID 109371; DOI: [10.1016/j.engstruct.2019.109371](https://doi.org/10.1016/j.engstruct.2019.109371).
- [31] T. Urban, M. Gołdyn, J. Krakowski, Ł. Krawczyk, "Experimental investigation on punching behavior of thick reinforced concrete slabs", *Archives of Civil Engineering*, 2013, vol. 59, no. 2, pp. 157–174; DOI: [10.2478/ace-2013-0008](https://doi.org/10.2478/ace-2013-0008).
- [32] P. Schmidt, D. Kueres, J. Hegger, "Contribution of concrete and shear reinforcement to the punching shear resistance of flat slabs", *Engineering Structures*, 2020, vol. 203, art. ID 109872; DOI: [10.1016/j.engstruct.2019.109872](https://doi.org/10.1016/j.engstruct.2019.109872).
- [33] M.H. Oliveira, M.J.M. Pereira Filho, D.R.C. Oliveira, et al., "Punching resistance of internal slab-column connections with double-headed shear studs", *Revista IBRACON de Estruturas e Materiais*, 2013, vol. 6, no. 5, pp. 681–714; DOI: [10.1590/S1983-41952013000500002](https://doi.org/10.1590/S1983-41952013000500002).
- [34] D.V. Bompá, A.Y. Elghazouli, "Structural performance of RC flat slabs connected to steel columns with shear heads", *Engineering Structures*, 2016, vol. 117, pp. 161–183; DOI: [10.1016/j.engstruct.2016.03.022](https://doi.org/10.1016/j.engstruct.2016.03.022).
- [35] B. Wieczorek, *Wewnętrzna strefa podporowa żelbetowego ustroju płytowo-słupowego w stanie awaryjnym wywołanym przebicciem płyty*. Gliwice, Poland: Wydawnictwo Politechniki Śląskiej, 2019.
- [36] M. Diao, Y. Li, H. Guan, et al., "Post-punching mechanisms of slab-column joints under upward and downward punching actions", *Magazine of Concrete Research*, 2021, vol. 73, no. 6, pp. 302–314; DOI: [10.1680/jmacr.19.00217](https://doi.org/10.1680/jmacr.19.00217).
- [37] A. Pinho Ramos, V.J.G. Lúcio, "Post-punching behaviour of prestressed concrete flat slabs", *Magazine of Concrete Research*, 2008, vol. 60, no. 4, pp. 245–251; DOI: [10.1680/macr.2008.60.4.245](https://doi.org/10.1680/macr.2008.60.4.245).
- [38] B. Wieczorek, "Influence of the location of the column on the load capacity of a slab-column connection for the inner column after punching", *Procedia Engineering*, 2013, vol. 57, pp. 1251–1259; DOI: [10.1016/j.proeng.2013.04.158](https://doi.org/10.1016/j.proeng.2013.04.158).
- [39] T. Urban, M. Gołdyn, "How To Strengthen Flat Slabs on Punching Shear – Traditionally With Steel or Innovative, By Using Fiber Composite Materials?", *Engineering Structures and Technologies*, 2019, vol. 11, no. 2, pp. 57–65; DOI: [10.3846/est.2019.10657](https://doi.org/10.3846/est.2019.10657).
- [40] M.F. Ruiz, A. Muttoni, J. Kunz, "Strengthening of flat slabs against punching shear using post-installed shear reinforcement", *Structural Journal*, 2010, vol. 107, no. 4, pp. 434–442.
- [41] T. Urban, J. Tarka, "Strengthening of slab-column connections with CFRP strips", *Archives of Civil Engineering*, 2010, vol. 56, no. 2, pp. 193–212; DOI: [10.2478/v.10169-010-0010-0](https://doi.org/10.2478/v.10169-010-0010-0).
- [42] D. Szczech, R. Kotynia, "Effect of shear reinforcement ratio on the shear capacity of GFRP reinforced concrete beams", *Archives of Civil Engineering*, 2021, vol. 67, no. 1, pp. 425–437; DOI: [10.24425/ace.2021.136481](https://doi.org/10.24425/ace.2021.136481).
- [43] M.D. Vanderbilt, "Shear Strength of Continuous Plates", *Journal of the Structural Division*, 1972, vol. 98, no. ST5, pp. 961–973.
- [44] T. Urban, *Nośność na przebicie w aspekcie proporcji boków słupa. Badania doświadczalne elementów i konstrukcji betonowych. Raport 3*. Łódź, 1994.
- [45] G.J. Milligan, M.A. Polak, C. Zurell, "Finite element analysis of punching shear behaviour of concrete slabs supported on rectangular columns", *Engineering Structures*, 2020, vol. 224, art. ID 111189; DOI: [10.1016/j.engstruct.2020.111189](https://doi.org/10.1016/j.engstruct.2020.111189).
- [46] M. Grabski, A. Ambroziak, "Influence of the shear cap size and stiffness on the distribution of shear forces in flat slabs", *Materials (Basel)*, 2022, vol. 15, no. 1; DOI: [10.3390/ma15010188](https://doi.org/10.3390/ma15010188).
- [47] M. Grabski, "Punching shear capacity in the connection of the slab to column topped with a head", Ph.D. thesis, Gdansk University of Technology, Poland, 2022.
- [48] *EN 1992-1-1 Eurocode 2: Design of concrete structures – Part 1-1: General rules and rules for buildings*. Brussels, Belgium: CEN (European Committee for Standardization), 2004.
- [49] *DIN EN 1992-1-1/NA:2011-01 Nationaler Anhang – National festgelegte Parameter – Eurocode 2: Bemessung und Konstruktion von Stahlbeton und Spannbetontragwerken. Teil 1-1: Allgemeine Bemessungsregeln und Regeln für den Hochbau*. DIBt (Deutsches Institut für Bautechnik), 2011.





- [50] *ACI 318-19 Building Code Requirements for Structural Concrete*. American Concrete Institute, Farmington Hills, MI, 2019.
- [51] FIB (International Federation for Structural Concrete), *fib Model Code for Concrete Structures 2010*. Ernst & Sohn, 2013.
- [52] K.-J. Bathe, E.N. Dvorkin, "A formulation of general shell elements—the use of mixed interpolation of tensorial components", *International Journal for Numerical Methods in Engineering*, 1986, vol. 22, no. 3, pp. 697–722; DOI: [10.1002/nme.1620220312](https://doi.org/10.1002/nme.1620220312).
- [53] J.D. Rodrigues, S. Natarajan, A.J.M. Ferreira, et al., "Analysis of composite plates through cell-based smoothed finite element and 4-noded mixed interpolation of tensorial components techniques", *Computers & Structures*, 2014, vol. 135, pp. 83–87; DOI: [10.1016/j.compstruc.2014.01.011](https://doi.org/10.1016/j.compstruc.2014.01.011).

## Bezpośrednia metoda weryfikacji przebicia poza głowicą słupa

**Słowa kluczowe:** przebicie, głowica, metoda bezpośrednia, płyta-słup, płyta żelbetowa

**Streszczenie:**

W artykule omówiono propozycję metody weryfikacji nośności na przebicie dużych podpór w oparciu o normę EN 1992-1-1. Przedstawiona metoda uwzględnia rzeczywisty rozkład sił ścinających w sąsiedztwie podpory z uwzględnieniem wpływu obciążeń niejednorodnych, nieregularnej geometrii stropu, koncentracji sił wewnętrznych w narożach podpory oraz wpływu zastosowanej sztywności głowy. Jest to kolejna zaleta proponowanej metody w porównaniu z normowymi metodami obliczania nośności na przebicie poza głowicami w połączeniu płyta-słup. Podsumowano wybrane aktualne normowe wytyczne dotyczące obliczania nośności na przebicie dla bardzo dużych podpór. Zaproponowaną metodę porównano z wybranymi normowymi metodami na przykładzie zaczerpniętym z praktyki projektowej. Autorzy niniejszej pracy mają nadzieję, że proponowana metoda będzie pomocna projektantom konstrukcji w ocenie rzeczywistej wytrzymałości na przebicie połączeń płyta-słup zwieńczonych głowicą. Metoda wykazała bardzo dobrą zgodność z przeprowadzonymi eksperymentami. Niemniej jednak wydaje się konieczne przeprowadzenie większej liczby badań laboratoryjnych w celu wykazania uniwersalności proponowanego podejścia. Opisana metoda bezpośrednia winna wzbudzić w środowisku inżynierów budownictwa i naukowców żywe zainteresowanie, które będzie polem do dyskusji i podjęcia tematu wyznaczania nośności na przebicie.

Received: 2022-04-08, Revised: 2022-06-13